PRediction Of Geospace Radiation Environment and Solar wind parameterS

Forecast of geomagnetic indices: needs and results

This project has received funding from the *European Union's Horizon 2020 research and innovation programme* under grant agreement No 637302.

Overview

- Introduction to geomagnetic indices
- Aims of PROGRESS
- Models
- Results

Current Systems

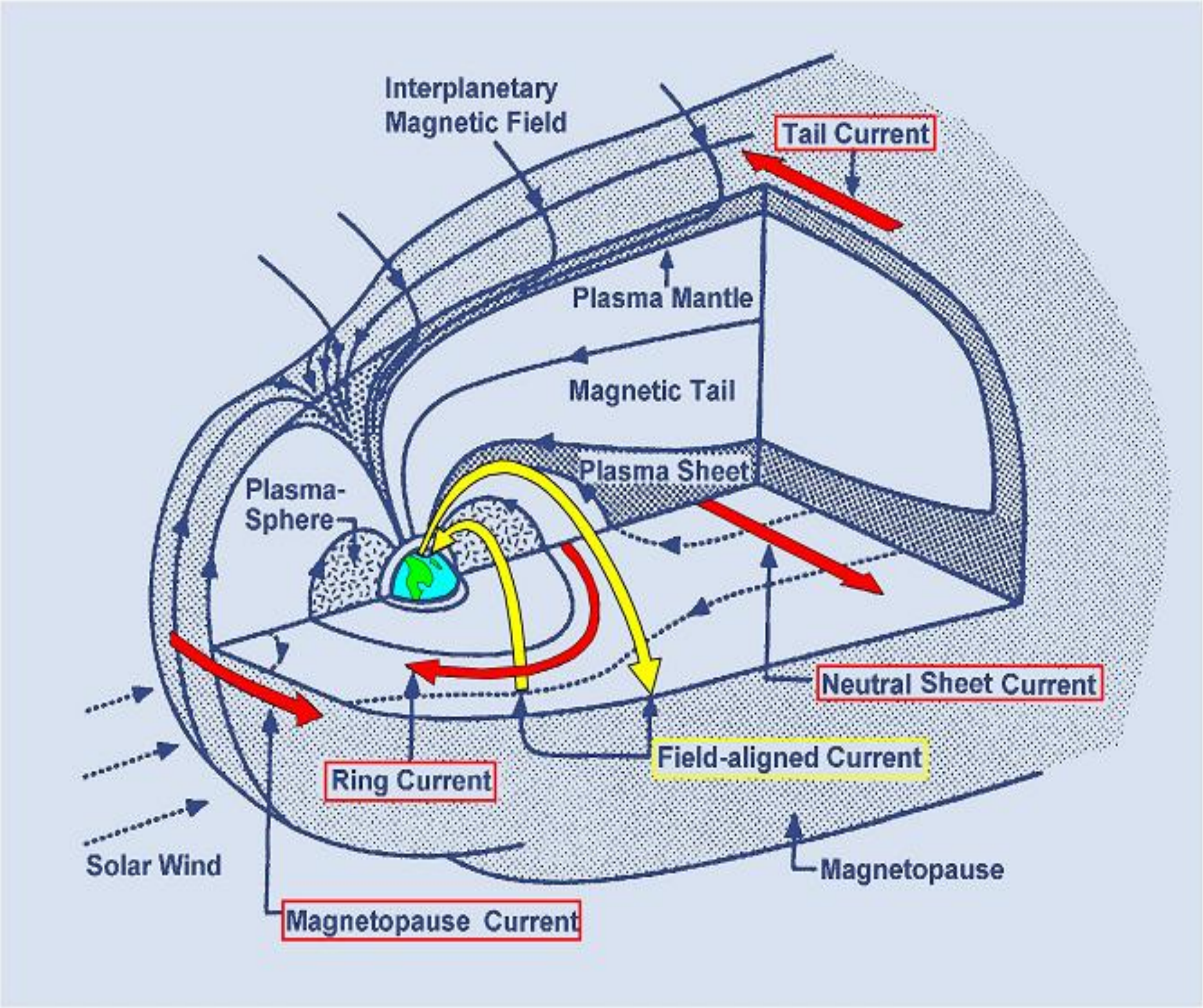

Introduction

Variation in terrestrial magnetic field

- Regular daily changes caused by regular solar radiation changes
- Irregular changes due to interactions in solar-magntospheric-ionospheric chain

Magnetic indices designed to describe variation of irregular current systems.

Examples of indices include Kp, Dst, AE

Kp

K-indices describe magnetic field variation with respect to quiet day (regular) variations at a single geomagnetic observatory

Kp is the mean, standardised K-index

- Computed from 13 stations
- Latitudes 44-60 degrees north or south

Designed to measure solar particle radiation

Dst

Disturbance Storm Time (Dst) index

- Measure of the intensity of the globally symmetrical equatorial electrojet or ring current
- Derived from near equatorial observatories

AE

Auroral Electroject index

Global, quantitive measure of auroral zone activity

Total deviation of horizontal magnetic field in the vicinity of the auroral oval

Used as a qualitative and quantitative correlative index to characterise substorm morphology

Uses

Indices are used to quantify geomagnetic activity in various magnetic latitude ranges

Used extensively in modelling

- Location of plasmapause

  $Lpp = 5.6 - 0.46\ Kp_{max}$

  (Carpenter and Anderson 1992)

- Radial diffusion coefficients

  $D_{LL} = 10^{0.056Kp - 9.325} L^{10}$

  (Brautigam and Albert 2000)

Sources

- GFZ Potsdam
  - http://www.gfz-potsdam.de/kp-index
- WDC Geomagnetism Kyoto
  - http://wdc.kugi.kyoto-u.ac.jp/wdc/Sec3.html
  - Dst, AE, Kp, AY/SYM
- WDC Geomagnetism Edinburgh
  - http://www.wdc.bgs.ac.uk/

PROGRESS

Objectives

- Develop new models for Kp, Dst, and AE
- Different methodologies
  - Neural networks (Lund)
  - NARMAX (Sheffield)
  - NARMAX + Lyapunov exponents (SRI)

- Results/forecasts available online
  - Graphical
  - Numerical

Assessment of forecasts

Assessment

$$\mathrm{MAE} = \frac{1}{n}\sum_{i=1}^{n}|e_i|$$

$$\mathrm{MSE} = \frac{1}{n}\sum_{i=1}^{n}e_i^2$$

$$\mathrm{RMSE} = \sqrt{\frac{1}{n}\sum_{i=1}^{n}e_i^2}$$

$$\mathrm{CORR} = \frac{\sum_i (x_i-\bar{x})(y_i-\bar{y})}{\sqrt{\sum_i (x_i-\bar{x})^2 \sum_i (y_i-\bar{y})^2}}$$

$$\mathrm{MSESS} = \frac{\mathrm{MSE}-\mathrm{MSE}_{\mathrm{ref}}}{\mathrm{MSE}_{\mathrm{perfect}}-\mathrm{MSE}_{\mathrm{ref}}} = 1-\frac{\mathrm{MSE}}{\mathrm{MSE}_{\mathrm{ref}}}$$

Kp - neural nets

	BIAS	MAE	RMSE	CORR	MSESS:PERS
Pers	-0.00	0.64	0.87	0.77	nan
IRF-Kp-2000	0.31	0.68	0.84	0.83	0.08
IRF-Kp-2017M	0.04	0.47	0.61	0.90	0.51
IRF-Kp-2017H	0.09	0.51	0.66	0.89	0.43
IRF-Kp-2017Kp	0.03	0.45	0.60	0.91	0.53

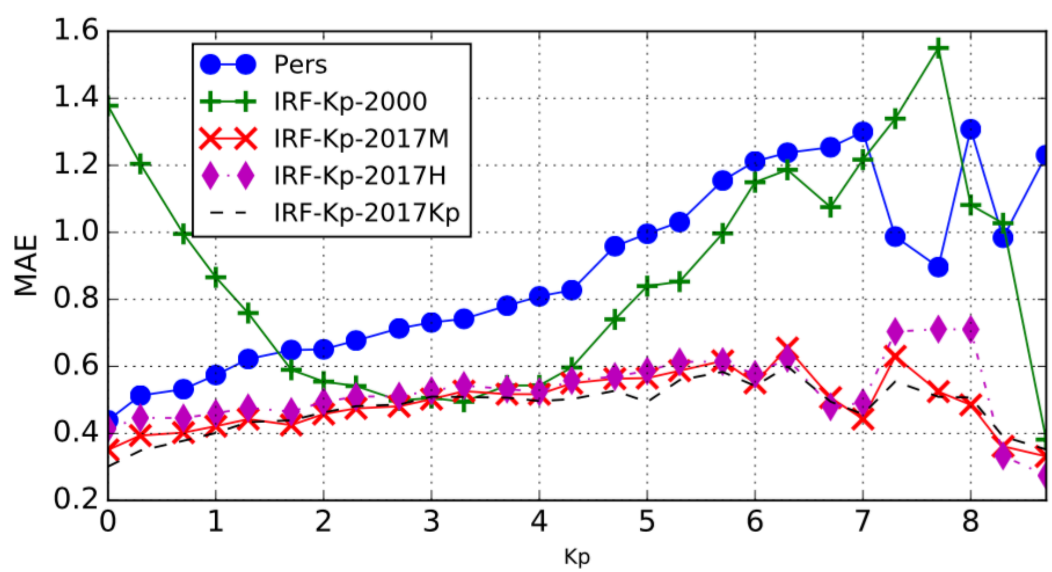

Forecasts

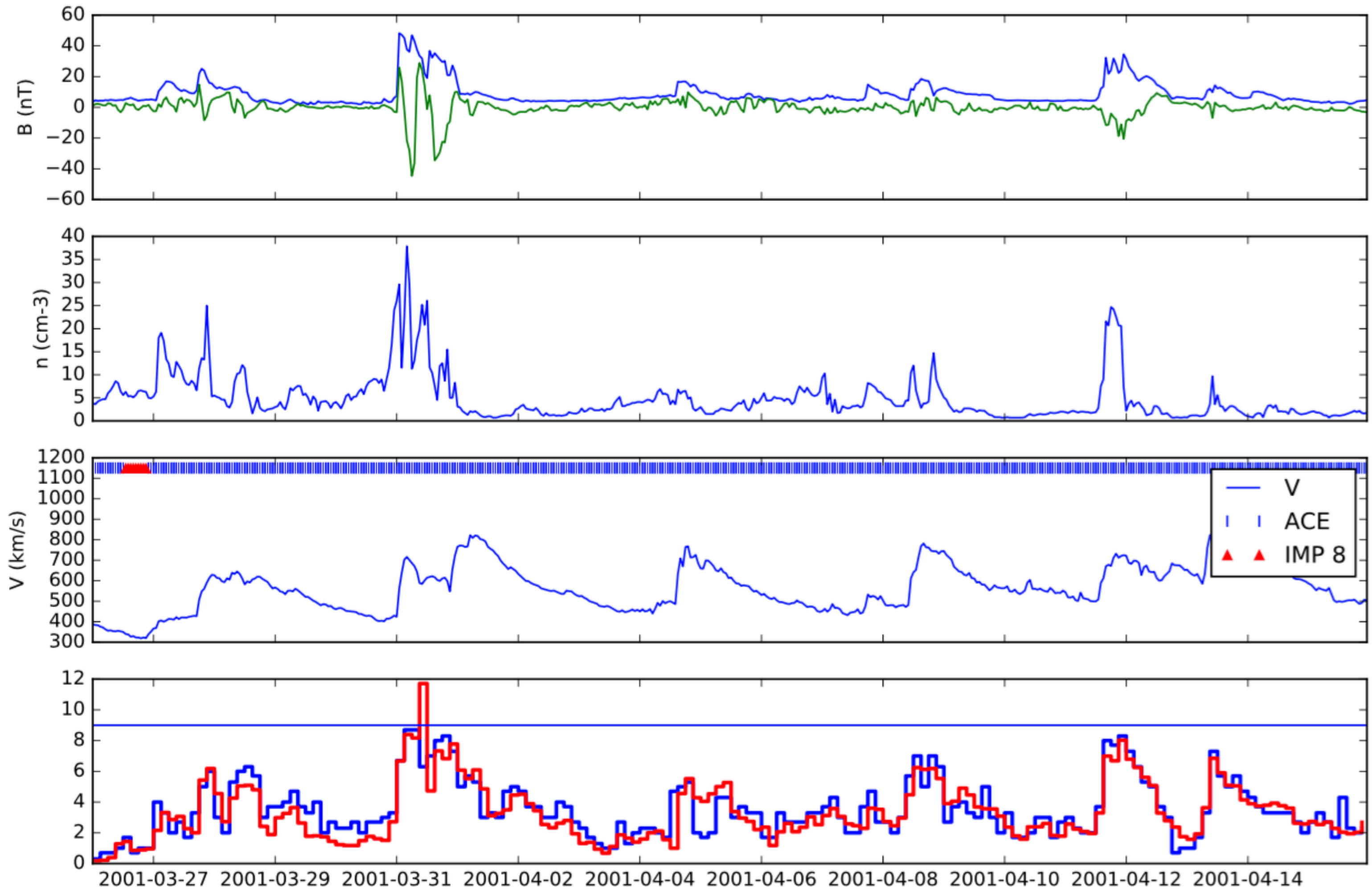

B (nT)
n (cm-3)
V (km/s)
V
ACE
IMP 8
2001-03-27 2001-03-29 2001-03-31 2001-04-02 2001-04-04 2001-04-06 2001-04-08 2001-04-10 2001-04-12 2001-04-14

Online forecast

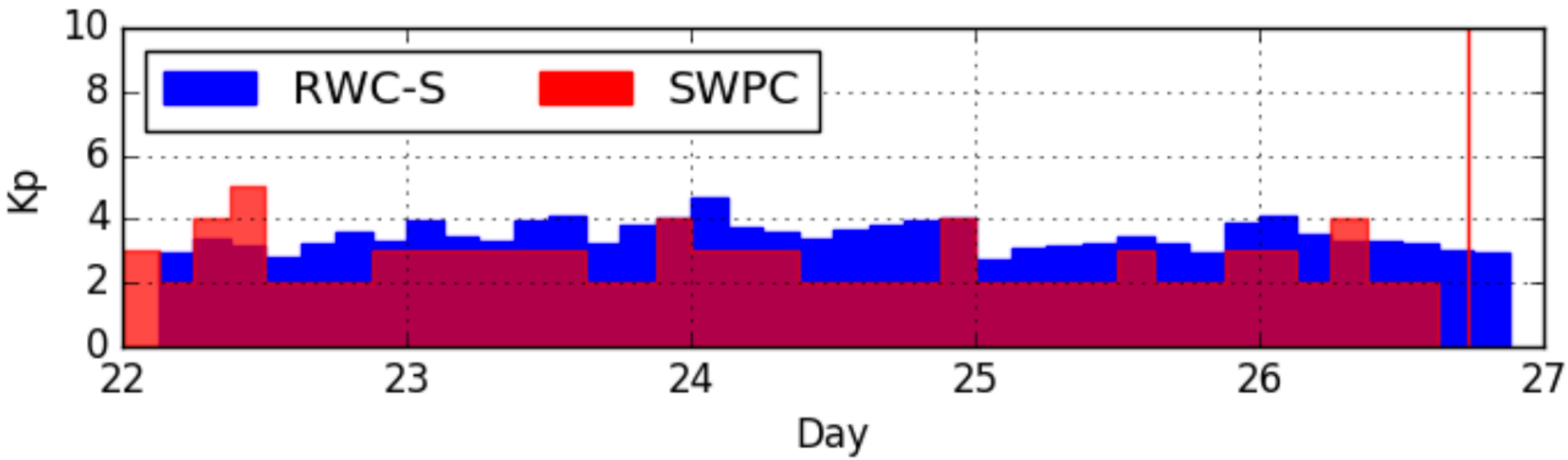

Kp- NARMAX

Inputs

- V - Solar wind speed
- Bs - Southward IMF component
- VBs – combination of above
- P – pressure and square root pressure

Output

Kp index

Four models generated providing forecasts of 3, 6, 12, and 24 hours

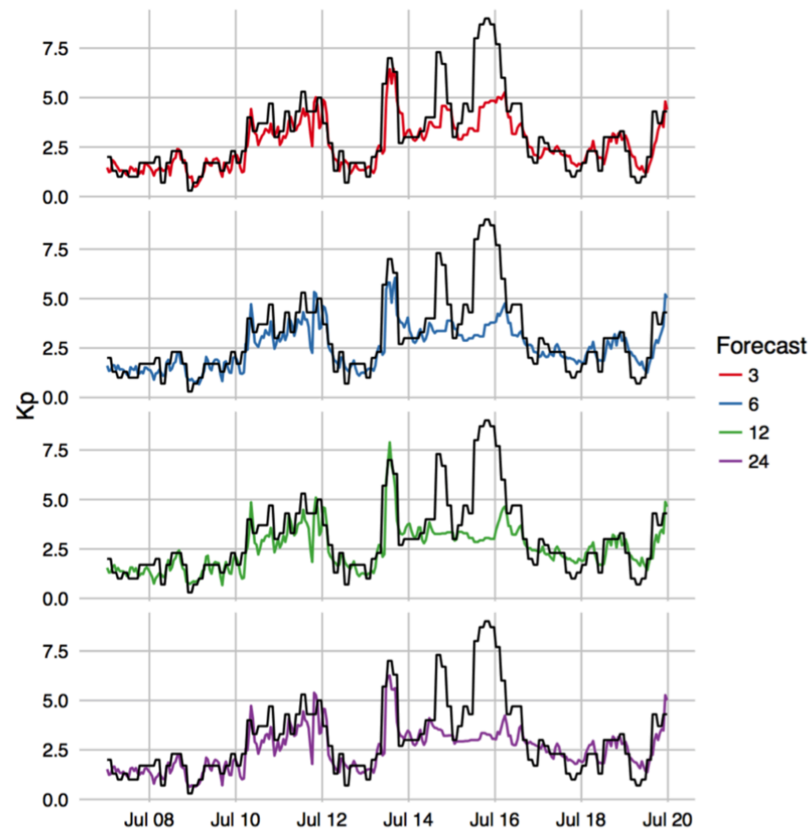

Dst Neural Net

- Employ time delay rather than recurrent network (mainly due to data considerations)
- Input data sets use velocity, density, magnetic field magnitude and y, z components
- Model improvements due to longer training data, larger network, and inclusion of |B| and By

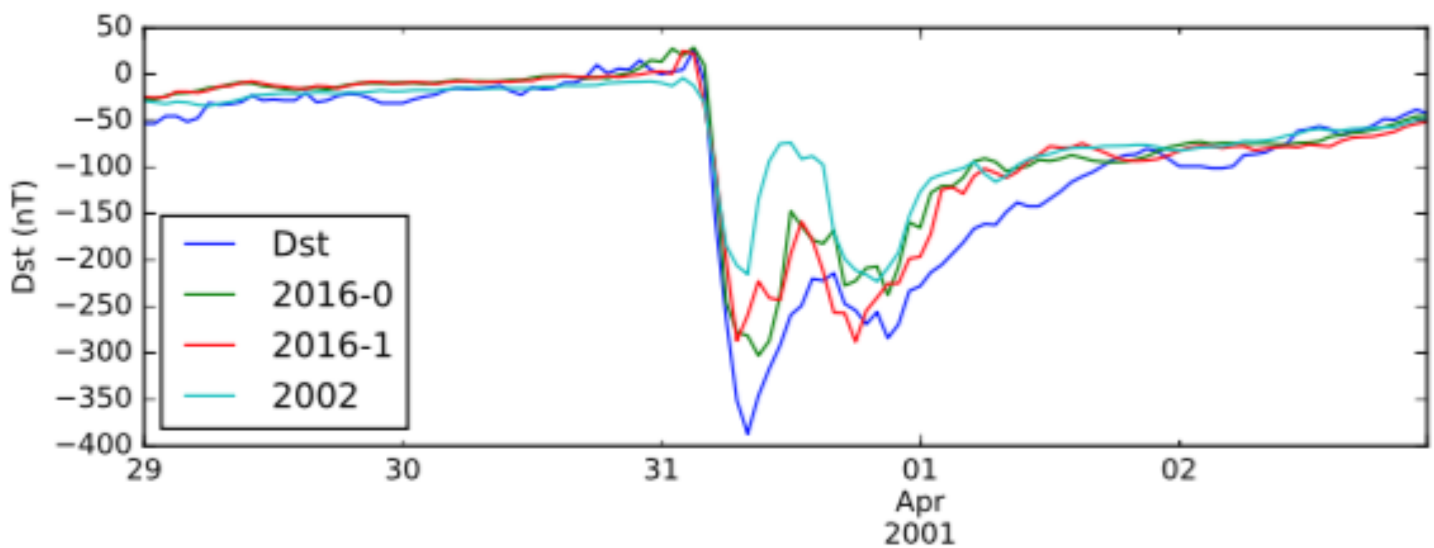

Dst Forecast

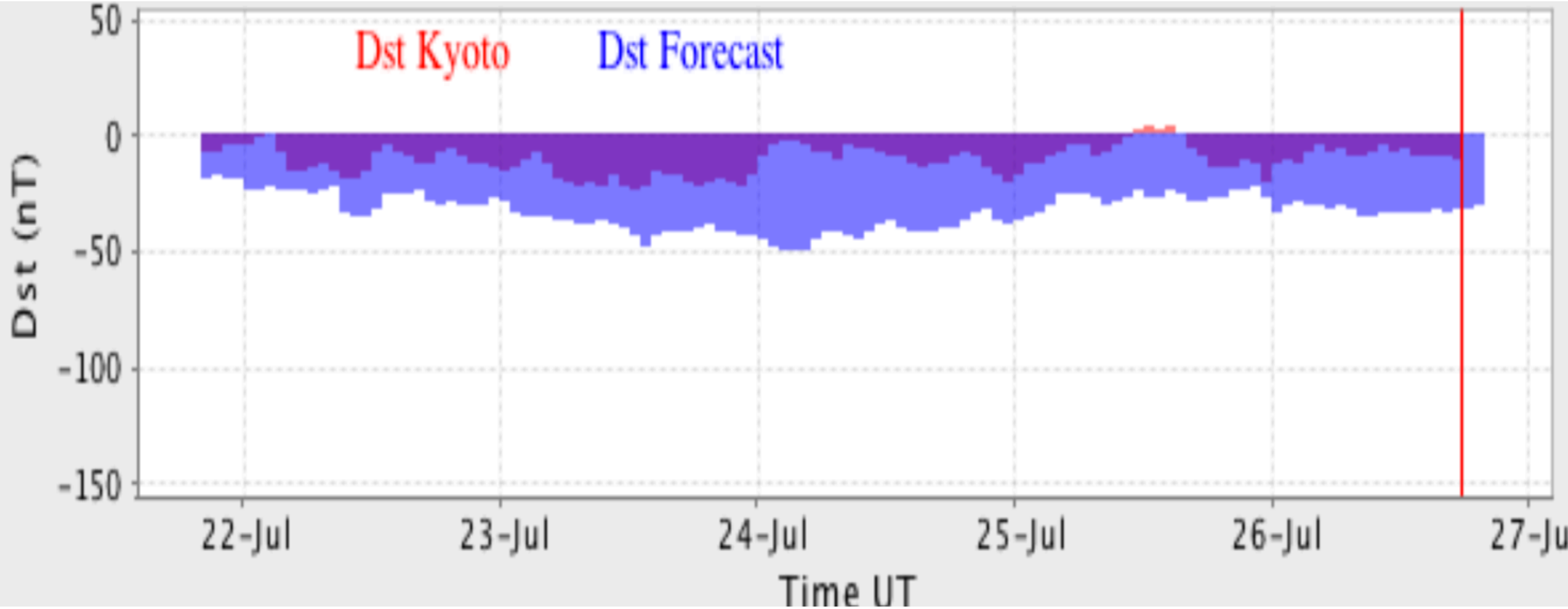

Dst NARMAX

Input - VBs
output Dst

Time interval : January-June 1979
(5 min resolution)

original data decimated to give 40 min and 1 h resolution

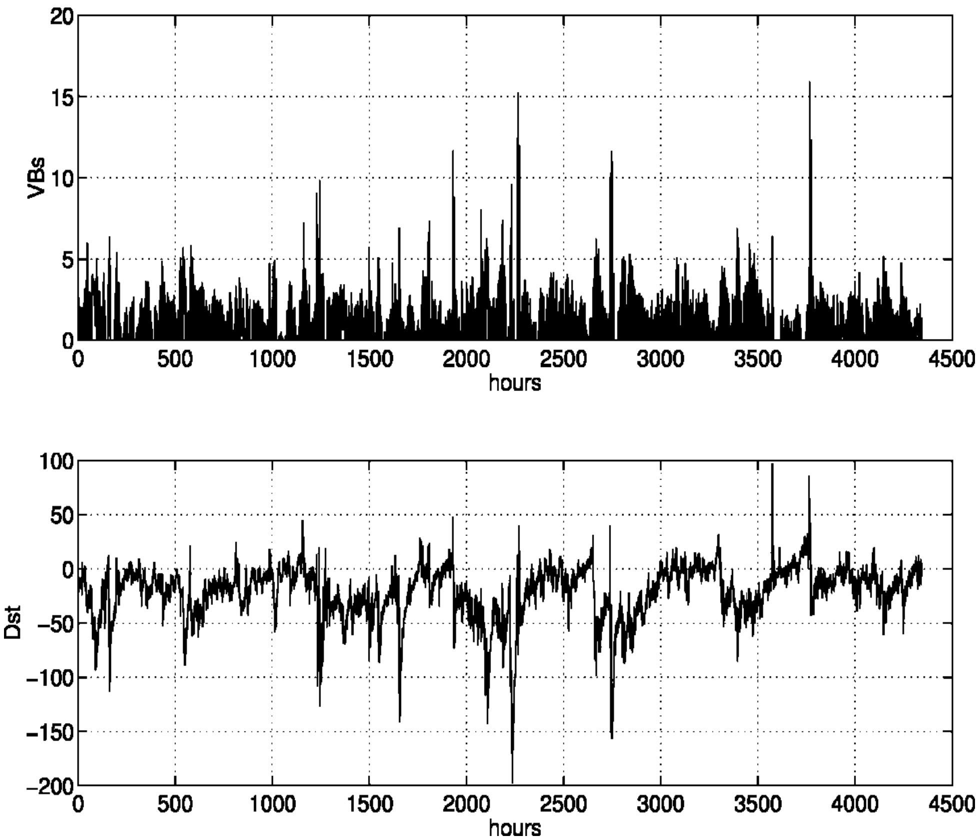

Dst 1 hour

$$D_{st}(k) = 1.18D_{st}(k-1) - 4.64VB_s(k-1) - 0.012D_{st}(k-2)VB_s(k-1) +$$
$$0.07D_{st}(k-3)VB_s(k-1) - 0.73D_{st}(k-2) + 0.67D_{st}(k-3) -$$
$$0.41D_{st}(k-4) + 0.19D_{st}(k-5) - 1.03VB_s(k-1)VB_s(k-6) +$$
$$0.93VB_s(k-2) + 0.96VB_s(k-1)VB_s(k-7) + 0.81VB_s(k-1)VB_s(k-13) -$$
$$0.67VB_s(k-3)VB_s(k-15) - 0.85VB_s(k-1)VB_s(k-8) +$$
$$0.31VB_s(k-3)VB_s(k-8)$$

Dst 1 hour forecast

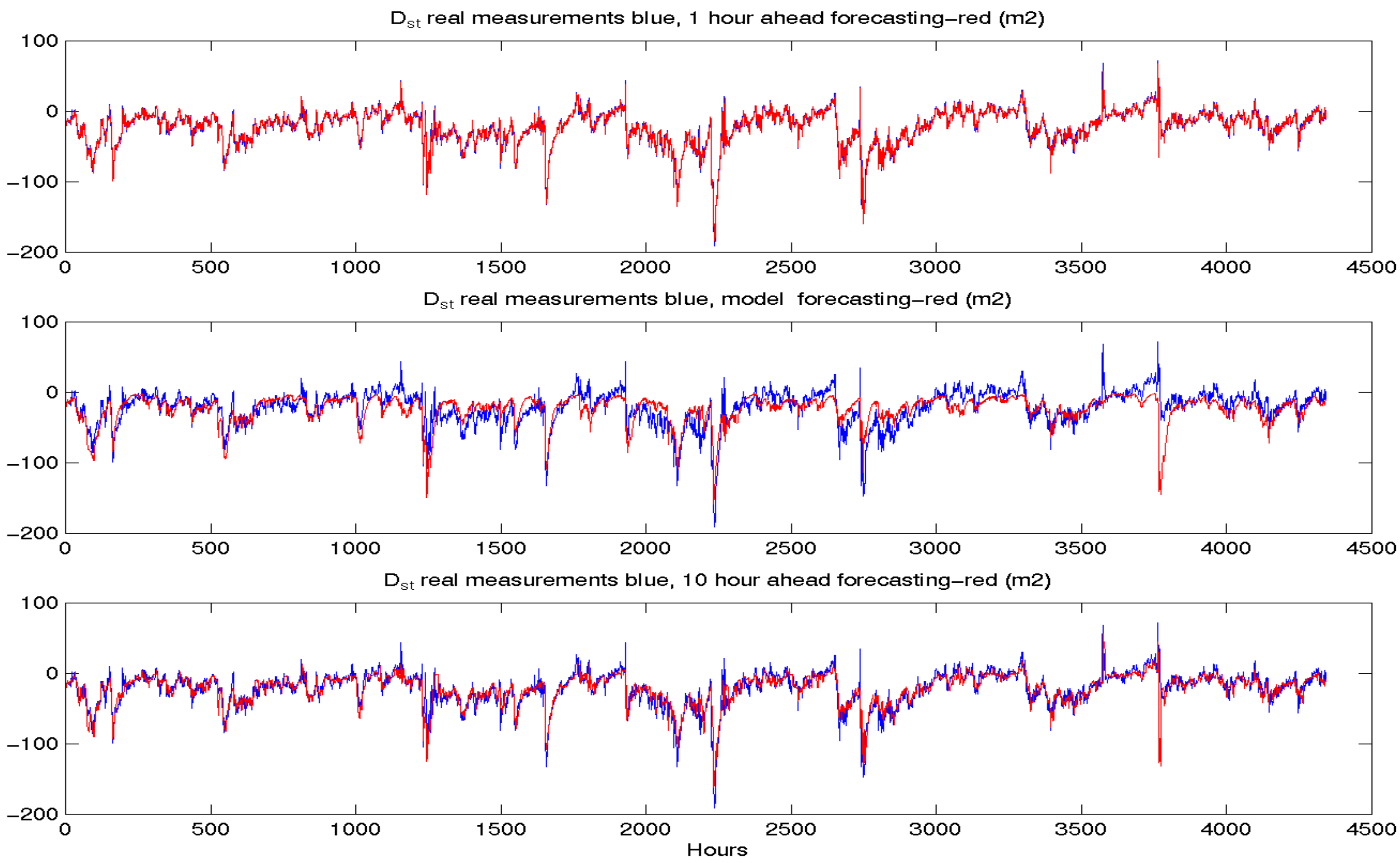

Analysis in the frequency domain
Second order transfer function $H_2(f_1, f_2)$

- Dominant ridge-like maximum:

$$f_1 + f_2 \to 0$$ Energy storage

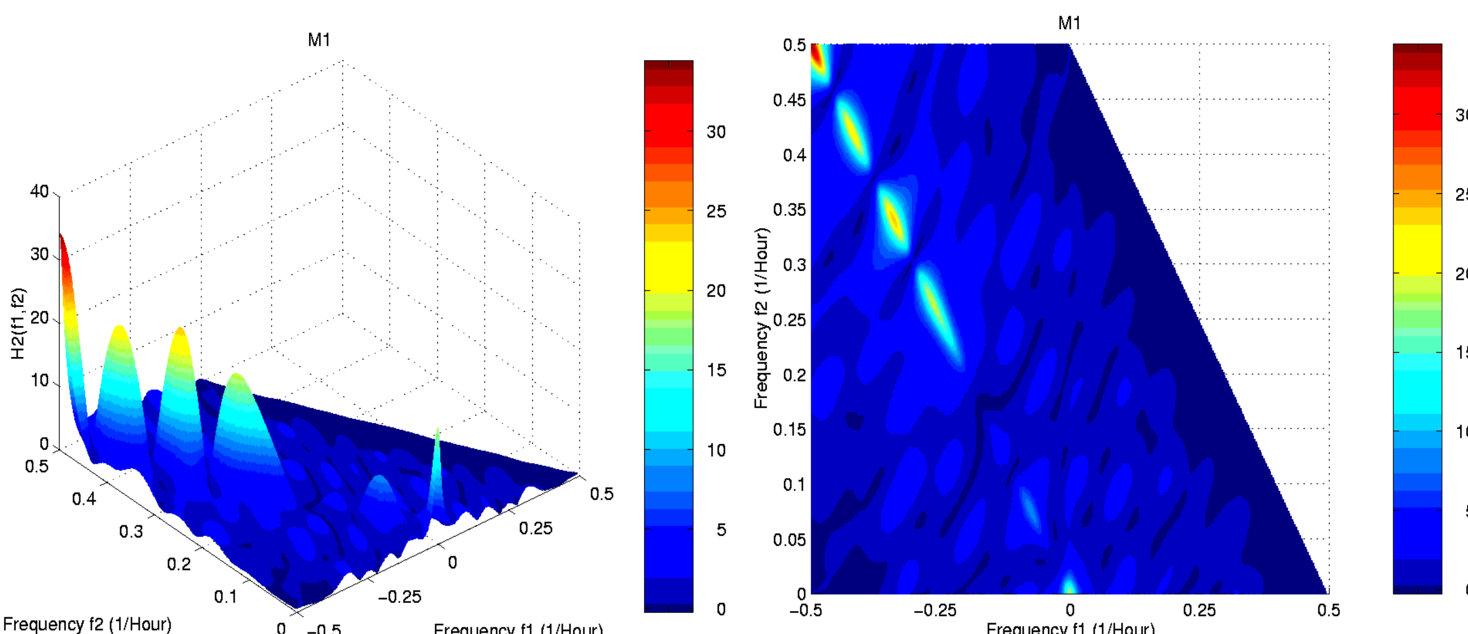

Figure 1:

The magnitude of H_2. Ridge-like maximum coresponds to
$f_1 + f_2 = 0$.

Analysis in the frequency domain
Second order transfer function $H_2(f_1, f_2)$

The University Of Sheffield.

Nonlinear Energy storage $f_1 + f_2 \to 0$

F_1 → [ ] → F_1 **Release time** $t_1 \sim 1/ F_1$

$F_1 + F_2$ → [ ] → $\delta F = F_1 + F_2$; $\delta F \ll F_1 + F_2$

Release time $t \sim 1/\delta F \gg t_1 ; t_2$

Another possibility: linear energy storage time delay for time t

$F(t_0)$ → [ ] → $F(t_{0+}t)$ **Linear Phase change in** H_1

Dst 40 minute resolution

$$D_{st}(k) = 1.16D_{st}(k-1) - 1.97VB_s(k-2) - 0.45D_{st}(k-2)$$
$$+ 0.25D_{st}(k-3) + 0.75VB_s(k-4) - 0.058VB_s(k-2)VB_s(k-6)^2$$
$$+ 0.29VB_s(k-2)VB_s(k-8) - 0.01VB_s(k-9)^3 - 0.03VB_s(k-3)^3 +$$
$$0.0035VB_s(k-5)^2VB_s(k-10) - 0.0047D_{st}(k-1)VB_s(k-2)^2$$
$$+ 0.033VB_s(k-6) + 0.0018D_{st}(k-3)VB_s(k-1)VB_s(k-4)$$
$$- 0.20VB_s(k-2)^2 + 0.012D_{st}(k-3)VB_s(k-2)$$

Dst 40 min forecast

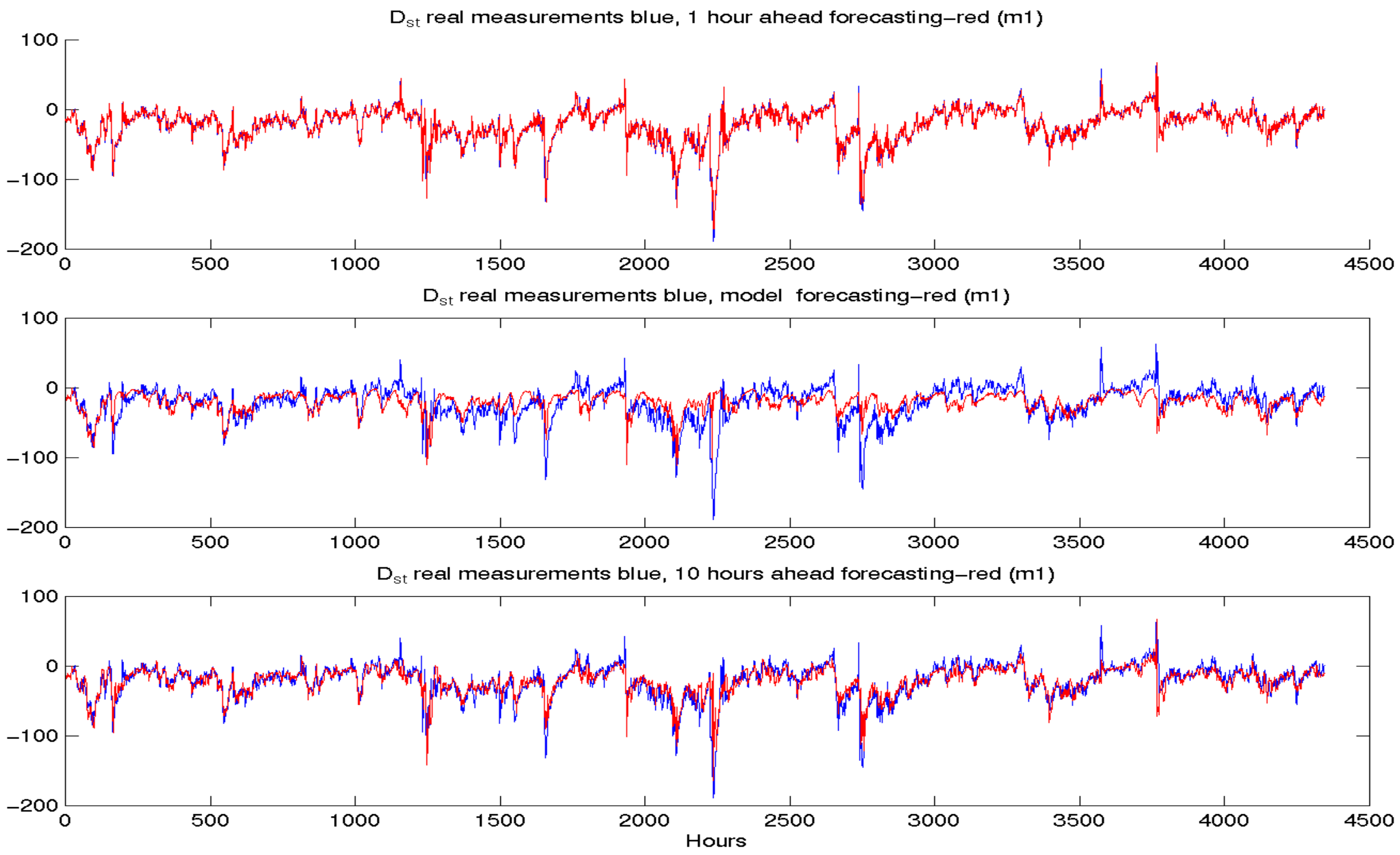

Analysis in the frequency domain
Second order transfer function $H_2(f_1, f_2)$

- Dominant ridge-like maximum $f_1 + f_2 \to 0$ Energy storage

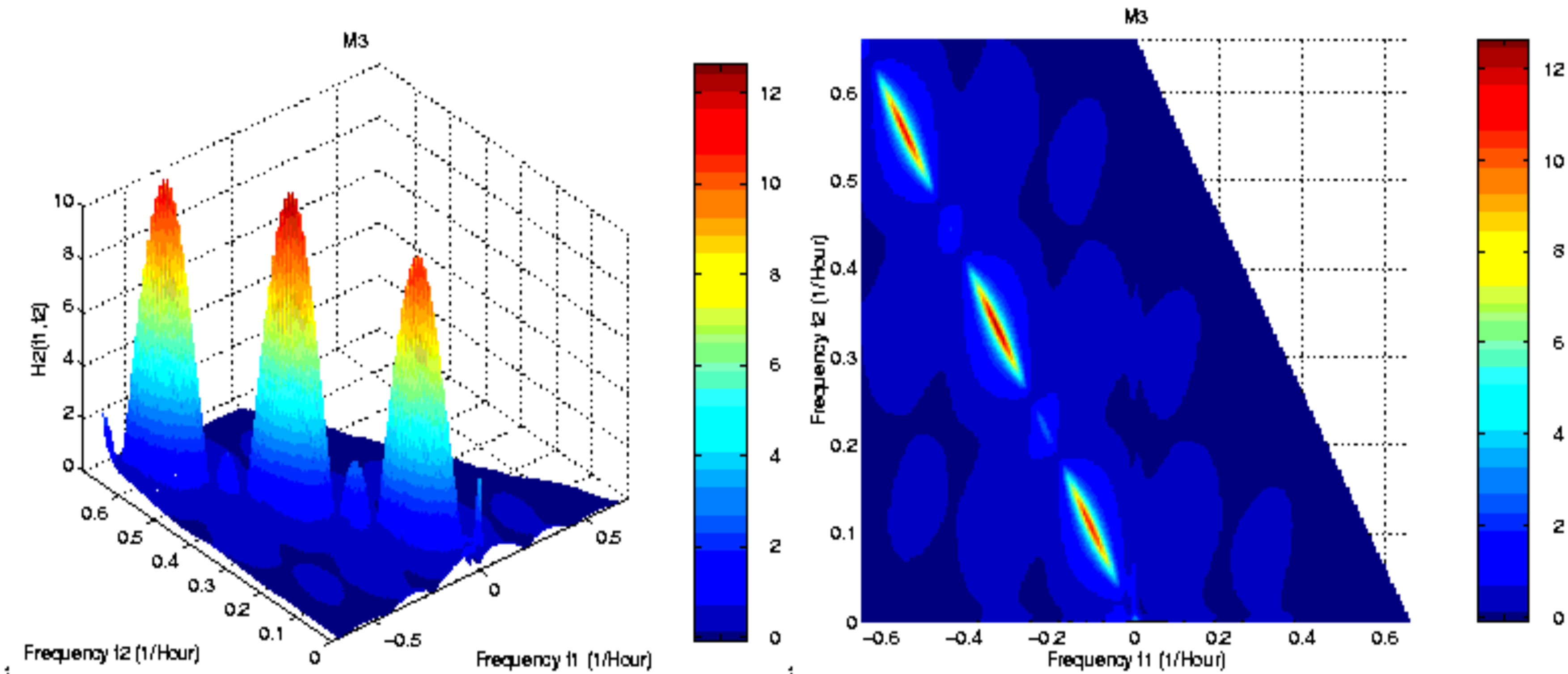

Figure 1:

Analytical approach to coupling functions

1. Burton et al 1975 VBs
2. Perreault and Akasofu [1974] $\varepsilon = VB^2 \sin(\theta/2)^4 l_0^2$,
3. Kan and Lee 1979

Solar Wind Magnetosphere "Coupling Functions"

The University Of Sheffield.

Name	Functional Form	Reference
B_z	B_z	*Dungey* [1961]
Velocity	v	*Crooker et al.* [1977]
Density	n	
p	$nv^2/2$	*Chapman and Ferraro* [1931]
Bs	B_z ($B_z < 0$); 0 ($B_z > 0$)	
Half-wave rectifier	vBs	*Burton et al.* [1975]
ε	$vB^2\sin^4(\theta_c/2)$	*Perrault and Akasofu* [1978]
ε_2	$vB_T^2\sin^4(\theta_c/2)$	Variant on ε
ε_3	$vB\sin^4(\theta_c/2)$	Variant on ε
Solar wind E-field	vB_T	
E_{KL}	$vB_T\sin^2(\theta_c/2)$	*Kan and Lee* [1979]
$E_{KL}^{1/2}$	$[vB_T\sin^2(\theta_c/2)]^{1/2}$	Variant on the Kan-Lee electric field
E_{KLV}	$v^{4/3}B_T\sin^2(\theta_c/2)p^{1/6}$	*Vasyliunas et al.* [1982]
E_{WAV}	$vB_T\sin^4(\theta_c/2)$	*Wygant et al.* [1983]
E_{WAV}^2	$[vB_T\sin^4(\theta_c/2)]^2$	Variant on E_{WAV}
$E_{WAV}^{1/2}$	$[vB_T\sin^4(\theta_c/2)]^{1/2}$	Variant on E_{WAV}
E_{WV}	$v^{4/3}B_T\sin^4(\theta_c/2)p^{1/6}$	*Vasyliunas et al.* [1982]
E_{SR}	$vB_T\sin^4(\theta_c/2)p^{1/2}$	*Scurry and Russell* [1991]
E_{TL}	$n^{1/2}v^2B_T\sin^6(\theta_c/2)$	*Temerin and Li* [2006]
$d\Phi_{MP}/dt$	$v^{4/3}B_T^{2/3}\sin^{8/3}(\theta_c/2)$	This paper

From Newell et al., 2007

Data based approach

Correlation function usually is a primary tool (e.g. Newell et al., 2007)

A04218 NEWELL ET AL.: PAIRS OF COUPLING FUNCTIONS A04218

Table 2. Various Possible Viscous Solar Wind Coupling Functions, Ranked According to Their Ability to Predict Variance in 10 Magnetospheric State Variables

Rank, f	Λ_c	Dst	AE	AU	Goes	Kp	Auro	b2i	Φ_{PC}	AL	$\Sigma r^2/n$
1. $n^{1/2}v^2$	−0.364	−0.500	0.469	0.430	−0.325	0.670	0.510	−0.520	0.319	−0.225	22.3%
2. $n^{1/3}v^2$	−0.371	−0.497	0.458	0.389	−0.353	0.678	0.512	−0.460	0.324	−0.250	21.8%
3. $n^{1/2}v^3$	−0.363	−0.517	0.452	0.383	−0.340	0.653	0.515	−0.449	0.317	−0.236	21.1%
4. $n^{1/6}v^2$	−0.353	−0.460	0.416	0.330	−0.347	0.628	0.471	−0.382	0.294	−0.254	18.5%
5. nv^3	−0.331	−0.507	0.425	0.421	−0.260	0.549	0.488	−0.516	0.272	−0.153	18.5%
6. $nv^{5/2}$	−0.312	−0.457	0.383	0.401	−0.239	0.525	0.448	−0.511	0.249	−0.124	16.3%
7. $v^{4/3}$	−0.374	−0.408	0.372	0.277	−0.321	0.547	0.402	−0.314	0.252	−0.250	14.7%
8. v	−0.324	−0.406	0.374	0.279	−0.321	0.537	0.399	−0.315	0.254	−0.251	14.7%
9. $v^{3/2}$	−0.321	−0.408	0.372	0.276	−0.319	0.549	0.404	−0.312	0.251	−0.249	14.7%
10. v^2	−0.317	−0.409	0.369	0.272	−0.311	0.547	0.407	−0.310	0.247	−0.246	14.4%
11. $v^{2/3}$	−0.325	−0.405	0.374	0.281	−0.311	0.503	0.396	−0.316	0.255	−0.252	14.4%
12. $v^{1/2}$	−0.325	−0.403	0.374	0.282	−0.294	0.465	0.395	−0.316	0.255	−0.252	14.0%
13. p	−0.277	−0.373	0.316	0.357	−0.202	0.469	0.391	−0.474	0.217	−0.085	12.5%
14. $p^{2/3}$	−0.272	−0.321	0.326	0.365	−0.199	0.486	0.377	−0.485	0.228	−0.101	12.4%
15. $p^{1/2}$	−0.267	−0.295	0.329	0.367	−0.194	0.482	0.366	−0.486	0.231	−0.108	12.2%
16. $p^{1/3}$	−0.193	−0.269	0.331	0.366	−0.186	0.463	0.353	−0.485	0.231	−0.115	11.7%
17. $p^{3/2}$	−0.274	−0.427	0.288	0.331	−0.183	0.394	0.397	−0.431	0.190	−0.057	11.1%
18. p^2	−0.257	−0.420	0.250	0.292	−0.150	0.288	0.387	−0.351	0.159	−0.031	8.5%
19. nv	−0.163	−0.149	0.143	0.221	−0.089	0.287	0.253	−0.325	0.136	0.004	4.0%
20. n	−0.041	0.030	0.001	0.093	0.033	0.103	0.122	−0.172	0.058	0.070	0.6%

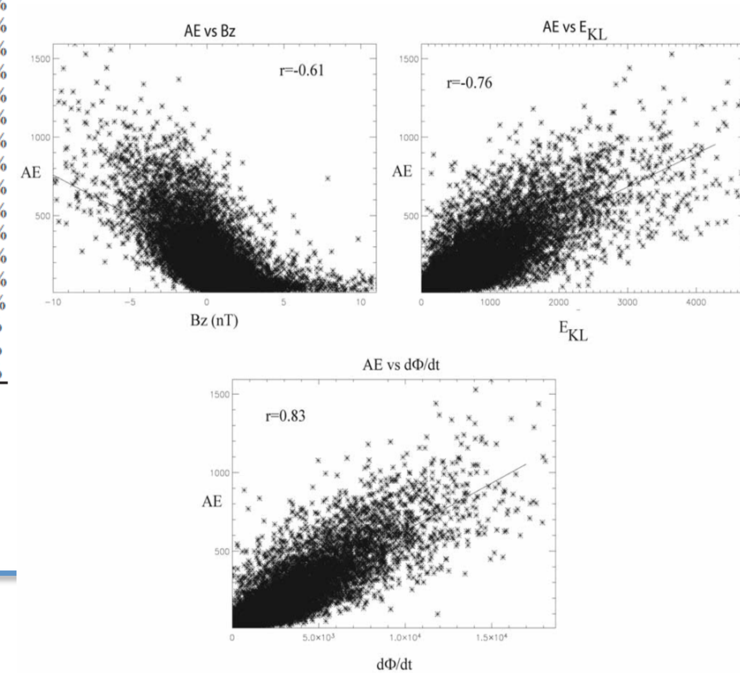

Solar Wind Magnetosphere "Coupling Functions"

X(t) → $y=x^2$ → Y(t)

5% Noise

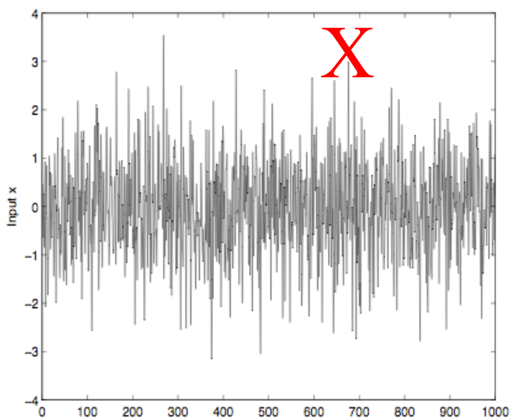

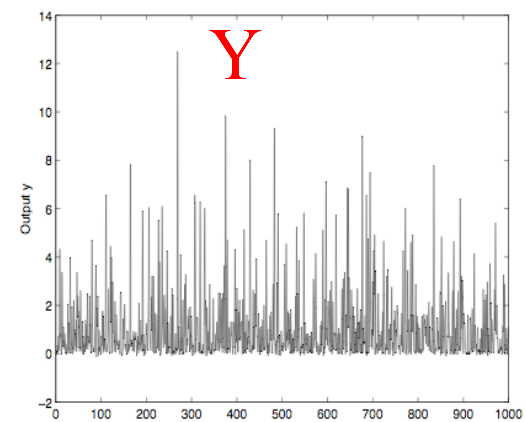

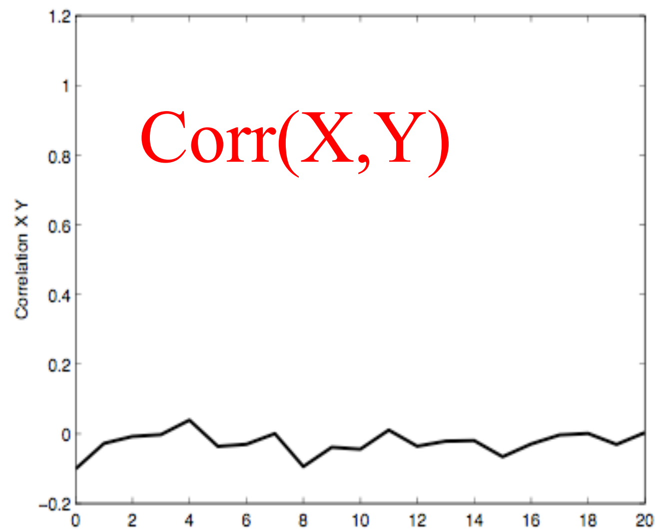

$$(X, Y)$$

$$(X^2, Y)$$

…………

$$(X^k, Y)$$

$$(X^{k+1}, Y)$$

……………

Coupling functions

1. $I_B = VB_s$ by *Burton et al.* [1975]
2. $\varepsilon = VB^2 \sin^4(\theta/2)$, by *Perreault and Akasofu* [1978]
3. $I_W = VB_T \sin^4(\theta/2)$ by *Wygant et al.* [1983]
4. $I_{SR} = p^{1/2} VB_T \sin^4(\theta/2)$ by *Scurry and Russell* [1991]
5. $I_{TL} = p^{1/2} VB_T \sin^6(\theta/2)$ by *Temerin and Li* [2006]
6. $I_N = V^{4/3} B_T^{2/3} \sin^{8/3}(\theta/2)$ by *Newell et al.* [2007]
7. $I_V = n^{1/6} V^{4/3} B_T \sin^4(\theta/2)$ by *Vasyliunas et al.* [1982]

Coupling Function	NERR
$p^{1/2} VB_T \sin^6(\theta/2)(t\text{-}1)$	31.32
$VB_s(t\text{-}1)$	12.76
$n^{1/6} V^{4/3} B_T \sin^4(\theta/2)(t\text{-}1)$	10.30
$p^{1/2} VB_T \sin^4(\theta/2)(t\text{-}1)$	8.37
$D_{st}(t\text{-}2)$	7.23

$p^{1/2}V^2B_T\sin^6(\theta/2)$	14.0
$p^{1/2}V^{4/3}B_T\sin^6(\theta/2)$	12.5
$P^{1/2}VB_T\sin^6(\theta/2)$	12.1
VB_s	8.91

$\sin^6(\theta/2)$ or $\sin^4(\theta/2)$?

Where $\sin^4(\theta/2)$ did appear from?

Kan and Lee (1978) model

The University Of Sheffield.

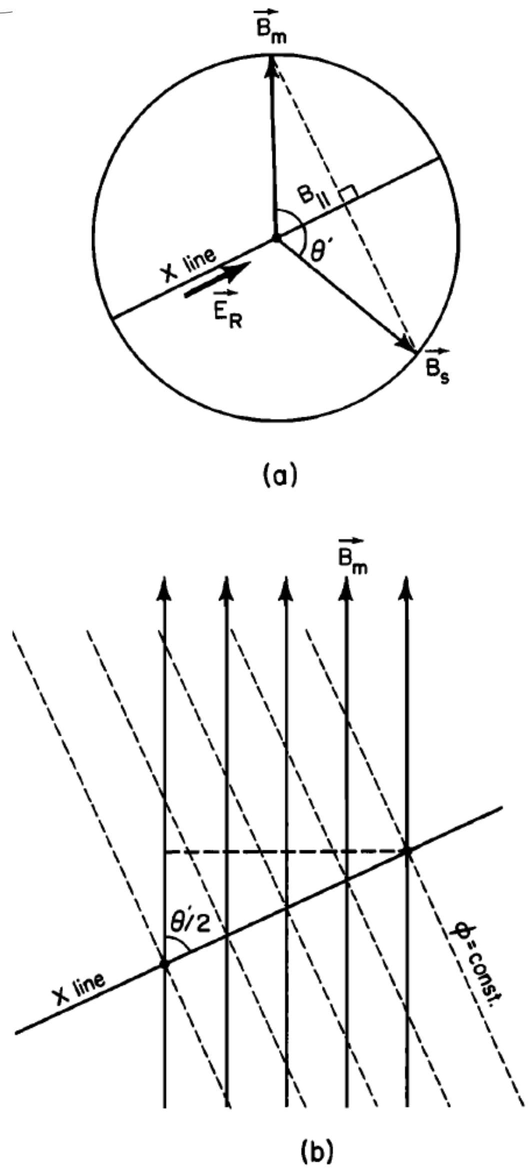

ig. 1. A schematic illustration of the field

$$E_R = V_s B_s \sin\left(\frac{\theta}{2}\right)$$

Reconnection Electric field for two magnetic fields of equal magnitudes:
Sonnerup (1974)
Russell and Atkinson (1973)

Kan and Lee stated that only perpendicular component of the electric field contributes to the potential across the polar

$$\Phi = \int E_{R\perp} dl_\perp = \int V_s B_s \sin^2\left(\frac{\theta}{2}\right) dl \sin\left(\frac{\theta}{2}\right)$$

$$\Phi = V_s B_s \sin^3\left(\frac{\theta}{2}\right) l_0$$

Finally Kan and Lee argued that power delivered by solar wind dynamo is proportional to potential square divided effective system resistance:

$$P = \frac{\Phi^2}{R} = V_s^2 B_s^2 \sin^6\left(\frac{\theta}{2}\right) l_0^2$$

ENERGY COUPLING FUNCTION AND SOLAR WIND—MAGNETOSPHERE DYNAMO

J.R. Kan and L.C. Lee

The University Of Sheffield.

The potential difference Φ_m across the polar cap is due to the perpendicular component of the reconnection electric field, i.e., $E_R \sin \theta/2$ as shown in Figure 1(b). This geometrical factor has been overlooked in the previous studies of component reconnection. Thus the polar cap potential Φ_m can be written as

$$\Phi_m = V_s B_s \sin^2 (\theta/2)\, \ell_o \qquad (3)$$

where ℓ_o is the effective length of the X line.

The power delivered by the solar wind dynamo is given by

$$P = \phi_m^2/R = V^2 B^2 \sin^4 (\theta/2)\, \ell_o{}^2/R$$

$$= (V/R)\ \varepsilon\,(t) \qquad (5)$$

Summary

- New models for Kp, Dst, and recently AE
- Plots of Dst, Kp forecasts available online from Lund or PROGRESS web site
- Other models will be added as they come online
- Access to numerical data will be available by the end of the project
- Systems methodologies can reveal physical processes